Available online at www.sciencedirect.com
SCIENCE DIRECT®
Journal of Nuclear Materials 336 (2005) 73–80
journal of nuclear materials
www.elsevier.com/locate/jnucmat

Experimental studies of mechanical properties of solid zirconium hydrides

M.P. Puls [a,*], San-Qiang Shi [b], J. Rabier [c]

[a] Fuel Channel and Materials Engineering Branch, Atomic Energy of Canada Limited, Sheridan Park Research Community, Mississauga, Ont., Canada L5K 1B2
[b] Department of Mechanical Engineering, The Hong Kong Polytechnic University, Hung Hom, Kowloon, Hong Kong
[c] Laboratoire de Métallurgie Physique, UMR 6630 CNRS-Université de POITIERS, SP2MI, BP 30179, F-86962 Chasseneuil Futuroscope cedex, France

Received 9 March 2004; accepted 31 August 2004

Abstract

Zirconium alloy Zr–2.5Nb has been hydrided to ZrH_x (x = 1.15–2.0), and studied using microhardness and unconfined and confined compression techniques. At room temperature, results on Young's modulus and yield strength of solid hydrides show that these mechanical properties remain about the same as the original zirconium alloy for hydrogen compositions up to about $ZrH_{1.5}$. The levels of these properties start to drop when δ hydride becomes the major phase and reaches a minimum for the ε hydride phase. Between room temperature and 300 °C, Young's modulus of solid hydrides decreases with temperature at about the same rate as it does for the original zirconium alloy.

1. Introduction

Knowledge of the mechanical properties of solid zirconium hydrides is important in the modeling of delayed hydride cracking (DHC) in zirconium alloys, which are important structural materials in the nuclear industry [1,2]. Using mostly compressive testing, Barraclough and Beevers [3,4], carried out an extensive study of the deformation behaviour of bulk zirconium hydride having stoichiometric composition, x = H/Zr, ranging from 1.27 to 1.92. They found that these bulk hydrides exhibited no or little plastic deformation at temperatures below 100 °C. In addition elastic properties such as Young's modulus were not measured. The reason for this may be partly due to the fact that it is difficult to prepare a defect-free, macrosized zirconium hydride specimen. The presence of these defects may contribute to the premature fracture of solid zirconium hydrides even in compression at low temperature. It was the intention of this work to test solid zirconium hydride specimens with stoichiometric compositions ranging from x = H/Zr of 1.2 to 1.9 on a microscale (smaller than a single grain size) using a microhardness indentation technique and compare these results with measurements on macrosized specimens using both confined and unconfined compression test techniques. These tests were carried out over a period of about five years from the late 1980s to the middle of 1990s between two laboratories, Laboratoire de Métallurgie Physique in Poitiers, France and AECL's Whiteshell Laboratory in Pinawa, Manitoba, Canada. Initially it was thought that

* Corresponding author. Tel.: +1 905 823 9060; fax: +1 905 403 7385.
E-mail address: pulsm@aecl.ca (M.P. Puls).

0022-3115/$ - see front matter © 2004 Elsevier B.V. All rights reserved.
doi:10.1016/j.jnucmat.2004.08.016

hydrostatic confinement was necessary for obtaining reliable data on the stress–strain behaviour of zirconium hydride at room temperature and possibly at higher temperatures, but later studies showed that reliable stress–strain behaviour could also be obtained from unconfined compression testing using carefully prepared zirconium hydride specimens. A limited number of the tests were carried out at temperatures up to about 400 °C.

2. Experimental procedure

Sections of Zr–2.5Nb pressure tube material were flattened and cut into small rectangular specimens (3 mm by 3 mm by 8 mm). Similar specimens were also produced from reactor-grade unalloyed Zr. These specimens were then hydrogenated to various hydrogen compositions ranging from x = H/Zr of ~1.2 to 1.9 in a modified Sieverts apparatus that was subsequently upgraded to a computerized hydriding facility. With the facility, vacuum is brought down to 1×10^{-7} Torr, the system is heated to 850 °C and then the system is slowly filled with high purity hydrogen (a few specimens were hydrogenated at a lower temperature of 600 °C) held at the maximum temperature for many hours then slowly cooled while decreasing the pressure to correspond to the desired H/Zr ratio. Initially difficulties were experienced in hydrogenating the specimens without introducing numerous fractures visible on the surfaces of the specimens; however, reducing the ingress rate of hydrogen into the specimen chamber and carefully controlling the cooling rate and hydrogen pressure during cooling eliminated this problem. In the upgraded facility, the hydrogen composition was controlled by monitoring hydrogen pressure by computer rather than manually as before. The stoichiometric composition of the hydrogen in the specimen was determined by measuring the weight gain of the specimen.

Confined compression tests were carried out mainly at room temperature with a few tests at 150 and 200 °C. The tests were carried out at the Laboratoire de Métallurgie Physique at the Université de Poitiers, Poitiers, France, using a machine that allowed for separate control of both the uniaxial compressive stress and the confining pressure by means of a solid medium for the confining pressure. This is the so-called Griggs machine, which was originally designed in the 1950s, an improved version of which was used for the present tests [5]. The first set of samples were deformed under a confining pressure of 1000 MPa. A lower confining pressure of 400 MPa was used in most of the remaining tests out of concern that the higher confining pressure could affect the accuracy of the results by creating friction stresses that would be too high. Only tests at ambient up to 200 °C were done under confinement. The strain rate was $2 \times 10^{-4}\,s^{-1}$. Initially the Griggs set up was used with the confining piston made of carbide having the same diameter as the surrounding jacket. Due to the friction generated by this confinement technique, the accuracy of this set up markedly decreases when the yield strength is much below 500 MPa, which it turns out to be for zirconium hydride at temperatures above ambient. Improvements were, therefore, made to this set up to handle the lower yield strength values by using a piston made of tungsten carbide having a diameter that is less than the surrounding jacket, thus reducing the friction due to the confinement. At above ambient temperatures, the specimens are also sufficiently ductile that they can be readily deformed into the plastic range without confinement. It further became evident that the ductility of ZrH_x of properly prepared specimens is such that even unconfined compressive deformation at ambient would give acceptable results. Therefore, the last sets of tests were done with an INSTRON 4002 mechanical testing machine at AECL's Whiteshell Laboratories that had been calibrated for compression testing against an ASTM standard with satisfactory results. Unconfined compression tests on solid hydrides of various compositions were performed with this machine at room temperature at a cross head speed of 0.1 mm/min (the same cross head speed as for the confined tests) which, for the 8 mm long specimens, translates to a strain rate of $2 \times 10^{-4}\,s^{-1}$.

Microhardness tests were done using a FISCHET H100 microhardness tester. This instrument was designed for use below 55 °C and is capable of evaluating the Young's modulus (E) of a material through the quantity, $E/(1 - \nu^2)$, where ν is the Poisson's ratio of the material. Since ν cannot be measured by this technique, and has not been determined by means of another technique, the Young's modulus determined from these tests is useful only for relative comparisons. In order to evaluate Young's modulus for hydrides at temperatures above 55 °C, a sample heater stage was designed using a new ceramic nose-piece and a sapphire indentor. This allowed us to evaluate the elastic modulus and hardness of specimens up to 300 °C.

3. Results and discussion

Metallography of hydrided, Zr–2.5Nb pressure tube material specimens shows a recrystallized, equi-axed grain structure which was produced as a result of the process of high temperature hydrogenation, for example, Fig. 1. Three zirconium hydride phases, γ, δ and ε, are known to form in the zirconium-hydrogen system. According to Moore and Young [6], at room temperature the single-phase δ hydride is formed at compositions between $ZrH_{1.60}$ and $ZrH_{1.64}$. Below $ZrH_{1.60}$, there is a mixture of γ and δ hydride phases plus α Zr.

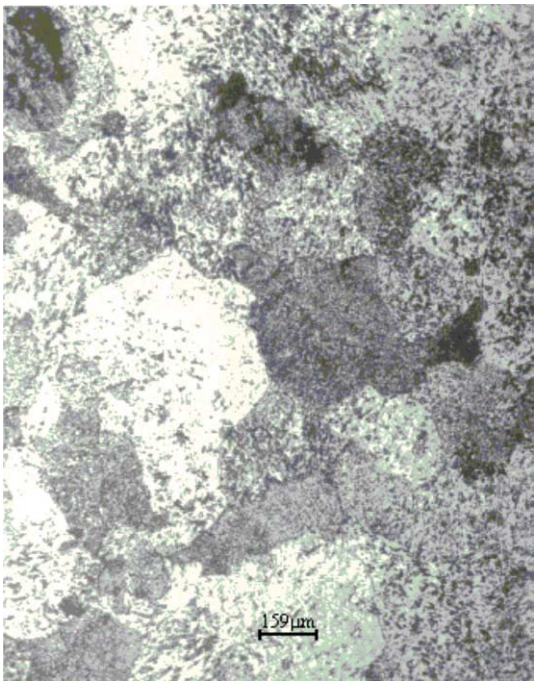

Fig. 1. The grain structure after hydriding to $ZrH_{1.8}$ starting from Zr–2.5Nb pressure tube material.

Between $ZrH_{1.64}$ and $ZrH_{1.74}$, there is a mixture of δ and ε hydride phases. Above $ZrH_{1.74}$, there is a single ε phase. Barraclough and Beevers [7] determined similar results but shifted to slightly lower H/Zr ratios. Thus they conclude that at room temperature the α + δ phase boundary is at $ZrH_{1.5}$ while the δ + ε phase boundary is at $ZrH_{1.61}$ and the ε phase boundary at $ZrH_{1.67}$. Barraclough and Beevers also conclude that the δ + ε field is not a true phase field but represents the difference in the martensitic start and completion temperatures, since the ε phase is formed from the δ phase by a martensitic transformation. Our metallographic examinations show microstructural features similar to those found by Barraclough and Beevers and consistent with these ranges of stoichiometric composition. Generally, after hydrogenation, the specimens appear to contain small microcracks in their interior, although it is not easy to distinguish cracks (or voids) from some other (unknown) microstructural feature.

The results of all the tests at various temperatures and stoichiometric composition $x = H/Zr$ are listed in Table 1. For the tests done under hydrostatic confinement, two types of stress–strain curves were obtained as shown in Fig. 2(a) and (b). One type shown in Fig. 2(a), found for samples with $1.3 < x < 1.62$, had high yield strengths with a fairly sharp transition between the elastic and the plastic deformation regime and little subsequent work hardening. The second type (Fig. 2(b)) had lower yield strengths, a more gradual transition between the elastic and the plastic regimes and strong work hardening. Deformation was generally stopped in these series of confined tests before any macroscopic fracture of the specimen. Yield strength was determined as the proportional limit, similar to what was used by Barraclough and Beevers [3,4].

Table 1
Yield strength versus stoichiometric composition, $x = H/Zr$, at different temperatures (confined tests below 400 °C)

Specimen no.	Stochiometry, x	Yield strength (MPa)
Temperature = ambient		
G232	1.00	622[a]
G223	1.12	633[a]
G170	1.21	751[a]
G142	1.21	794[a]
G225	1.25	636[a]
G165	1.37	870[b]
G140	1.43	968
G167	1.48	893[b]
G226	1.57	721[a,b]
G224	1.61	746[a,b]
G166	1.62	817[b]
G141	1.66	990
G168	1.67	607
G163	1.69	685
G145	1.69	503
G144	1.81	715
G230	1.83	431[a]
G231	1.86	529[a]
G169	1.89	672
G164	1.95	629
Temperature = 150 °C		
G211	1.30	646
G212	1.94	348
Temperature = 200 °C		
G235	1.15	170[a]
G236	1.58	122[a]
G234	1.90	185[a]
Temperature = 400 °C		
I5	1.21	118[a]
I6	1.43	158
I4	1.61	191
I2	1.72	88
I7	1.96	110
Temperature = 410 °C		
I15	1.15	150
I12	1.40	174
I11	1.57	192
I14	1.69	202
I10	1.91	140

All samples were hydrogenated at 850 °C from Zr–2.5Nb pressure tube material, except where otherwise indicated.
[a] Made from reactor grade Zr.
[b] Hydrogenated at 600 °C.

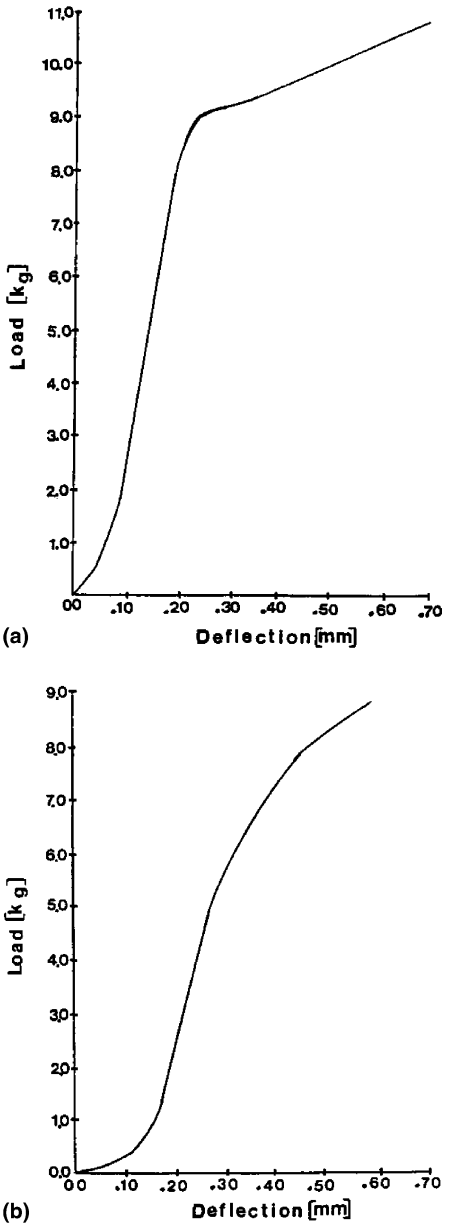

Fig. 2. (a) One type of load–deflection curve for specimens with $1.3 < x < 1.62$ and deformed under confinement in the Griggs machine showing a fairly sharp transition between the elastic and the plastic deformation regime and little subsequent work hardening. (Specimen G167 with $x = 1.48$; the vertical axis has been divided by 100.) (b) One type of load–deflection curve for specimens $x > 1.62$ or $x < 1.3$ and deformed under confinement in the Griggs machine showing a gradual transition between the elastic and the plastic regimes and strong work hardening. (Specimen G168 with $x = 1.68$.)

The yield strength results are plotted as a function of x in Fig. 3 for tests at various temperatures. Fig. 3 also contains a comparison of our results at 400 °C with the

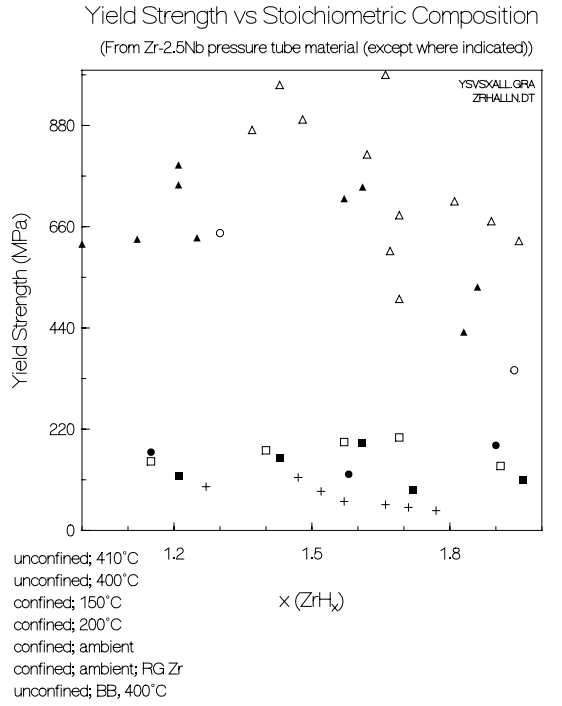

Fig. 3. Yield strength (proportional limit) versus stoichimetric composition, x = H/Zr, tested at temperatures indicated in the legend. In the legend, 'RG Zr' refers to reactor grade Zr starting material, 'confined' means tests carried out with the Griggs machine under hydrostatic stress, 'unconfined' refers to uniaxial tests carried without any confining hydrostatic pressure and BB refers to results obtained by Barraclough and Beevers [3,4].

corresponding results of Barraclough and Beevers [3,4]. Fig. 4 is a plot of the temperature dependence of these yield strength data for various x, where the data listed in Table 1 have been rounded to the nearest integer, averaging the yield strength values falling into each rounded value of x. This figure shows that there is a sharp drop in yield stress from ambient to 150 °C with a much more gradual decrease to 400 °C after that. The two figures show that Barraclough and Beevers's results are consistently lower than ours at all temperatures. Our results show that the highest yield strength values are found just below a stoichiometric composition of $x \sim 1.7$. There appears to be a large drop (minimum) in yield strength value at $x \sim 1.7$ and a gradual rise beyond that. Barraclough and Beevers's results show a decrease at a composition of $x \sim 1.5$ that continues to their maximum composition measured of $x \sim 1.78$. The difference cannot be due to the composition of the starting material since we obtain comparable yield strength values for the same stoichiometric composition regardless of whether the starting material is Zr–2.5Nb pressure tube material or reactor-grade, unalloyed Zr. The difference in the results may be in the grain size of our

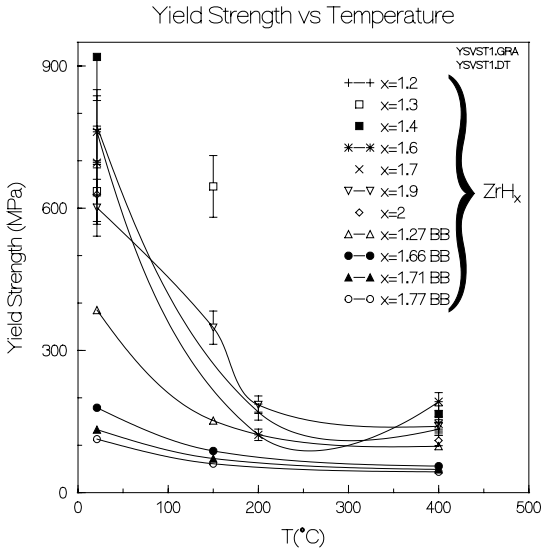

Fig. 4. Yield strength versus temperature for solid zirconium specimens of different stoichiometric composition. In the legend, BB refers to results obtained by Barraclough and Beevers [3,4]. A spline fit was used to connect the points when data for three or more temperatures at a given x were available.

specimens which was smaller than in the specimens from unalloyed Zr by Barraclough and Beevers. However, our hydride specimens produced from reactor grade zirconium had grain sizes similar to those found by Barraclough and Beevers. More likely, the difference is due to the scatter in our data. Thus, as a result of averaging the yield strength values over the nearest tenth of the stoichiometric composition, the results plotted in Fig. 4 show that the highest yield strength is at $x = 1.4$–1.5.

A set of cumulative deformations starting at ~400 °C and decreasing in steps to ambient were carried out for specimens of different stoichiometric composition and the results are listed in Table 2 and plotted in Fig. 5. Such an experimental approach has the advantage that there is no variation (or uncertainty) in x for specimens tested at different temperatures. The results are qualitatively similar to those of Fig. 4. However, the reduction in yield strength with temperature is greater for the non-cumulative tests. The lower reduction in yield strength with temperature for the cumulative tests is likely because the cumulative deformation at progressively lower temperatures results in yield strength values that are progressively greater than they would be in a corresponding non-cumulative test. The yield strength values at lower temperatures in these cumulative tests are therefore likely greater than if a single yield strength measurement at each temperature with a different specimen had been carried out. The yield strength for the cumulative test at $x = 1.77$ stands out, being much smaller than

Table 2
Yield strength (proportional limit) versus temperature for solid hydrides of different stoichiometric composition, $x = H/Zr$ (cumulative, unconfined tests)

Yield strength (MPa)	Temperature (°C)
$x = 1.23$ (specimen no. 14D)	
545	57
362	112
276	185
240	303
204	392
$x = 1.50$ (specimen no. 11G)	
486	63
344	129
284	213
255	412
$x = 1.54$ (specimen no. 12B)	
545	54
326	117
308	187
284	295
213	394
$x = 1.77$ (specimen no. 9E)	
328	20
273	59
218	120
162	195
90	410
$x = 1.92$ (specimen no. 15D)	
551	26
442	56
375	116
340	211
301	308

those with x values greater and less than 1.77. This is in qualitative agreement with the results from the non-cumulative tests (Fig. 3) that also show a minimum in yield strength in that range of x.

Fig. 6 summarizes the room temperature results of microhardness tests using a diamond indentor. Tests were conducted on the axial–transverse plane corresponding to the original tube material. One can see from Fig. 6 that the effective Young's modulus of solid hydrides starts to drop when the δ hydride phase dominates and that the modulus reaches a minimum level when the specimens consist entirely of ε phase. This result is largely in agreement with that found by Barraclough and Beevers [7], although our results show a less abrupt drop in the modulus quantity $E/1 - v^2$ compared to the microhardness value from which this quantity is derived. Large scatter in the data for measurements on different grains is also evident. It may be that different grains have different hydrogen compositions, or, more likely, different orientations may deform differently.

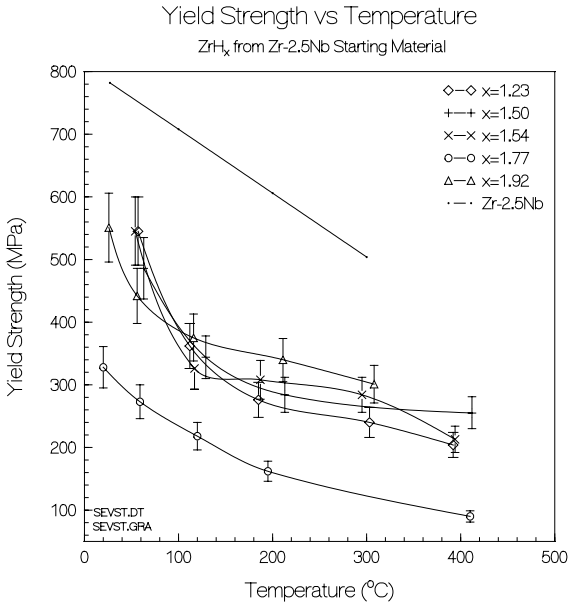

Fig. 5. Yield strength versus temperature obtained by cumulative deformation of each sample with a given stoichiometric composition, starting at the highest temperature. The solid line for Zr–2.5Nb is the mean value for the temperature dependence of unirradiated cold-worked Zr–2.5Nb pressure tube material deformed in the transverse pressure tube direction.

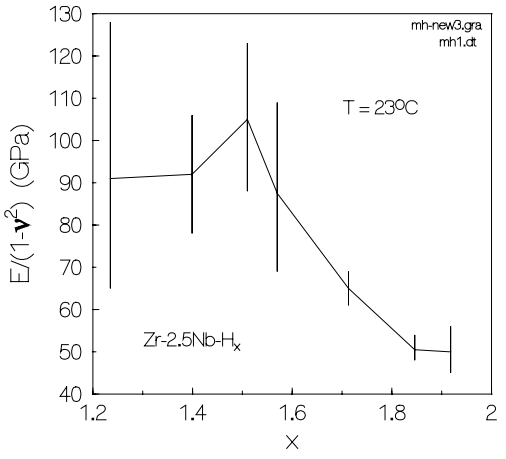

Fig. 6. The apparent Young's modulus of solid hydrides at room temperature from microhardness tests using a diamond indenter.

Microhardness tests at elevated temperatures were performed using a sapphire indentor. Since the computer program supplied by the manufacturer for data acquisition and data analysis is not made for such an indentor, the absolute values of $E/1-v^2$ obtained from these measurements were not calibrated for by the manufacturer for the tests at elevated temperatures. Therefore, the $E/1-v^2$ values should be considered as nominal values only, showing mainly their variations with temperature. Fig. 7 gives three examples. It can be seen from this figure that the nominal $E/1-v^2$ decreases with increase in temperature and that the effect of more hydrogen is merely to shift the lines of $E/1-v^2$ to lower levels, while the rate of change is about the same as for the original zirconium alloy, although the data of $E/1-v^2$ for high hydrogen composition show a tendency of curvature with temperature.

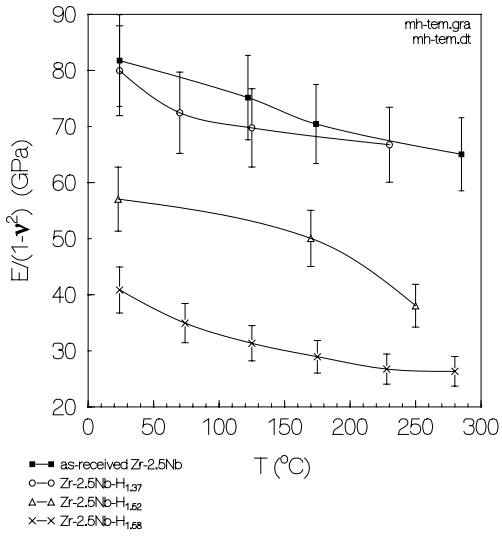

Fig. 7. The apparent Young's modulus, $E/(1-v^2)$, of solid hydrides at elevated temperatures from microhardness tests using a sapphire indenter. A spline fit was used to connect the data.

Table 3
Yield strength (proportional limit) versus stoichiometric composition, x = H/Zr, for unconfined tests at ambient temperature

Specimen no.	x	Yield strength (MPa)
ZrH14A-C	1.4	606
ZrH15A,D,E	1.5	539
ZrH16A-C	1.6	630
PT16C-2	1.65	669
ZrH17A-D	1.7	327
PT16A-1	1.74	389
T1PT6-2	1.75	295
T1PT6-1	1.76	201
ZrH18A-D	1.8	255
ZrH19A-D	1.9	266
ZrH20A-B	2	197

As an continuation of the initial work on constrained compression tests of solid hydrides, a new unconstrained compression test facility was set up. This facility was used to determine the Young's modulus and yield strength of solid zirconium hydrides at room tempera-

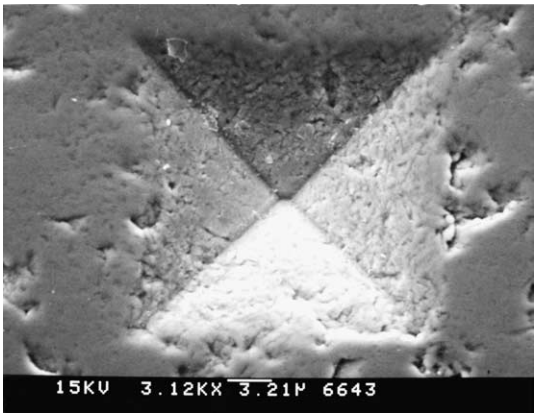

Fig. 8. SEM image of an indentation on the solid hydride specimen $ZrH_{1.8}$.

ture. For each hydrogen composition, three specimens were tested. Table 3 lists the results for yield strength. All hydrided specimens were deformed to failure of the specimen, which failed by fracturing into small pieces. The specimens with higher hydrogen compositions show some ductility, but still are very brittle compared to the non-hydrided, as-received material. Metallography revealed a porous-like structure (Fig. 8) for specimens with high hydrogen compositions, which might have contributed to the apparent ductility. Fig. 9 shows how the stress–strain behaviour varied with x. The deformation curves obtained show a similar trend with x as obtained with the confined tests; i.e., the curves for compositions $x = 1.4$–1.6 having high yield and a sharper transition to a limited work hardening stage beyond yield. This shows that the most brittle behaviour is exhibited at compositions where δ hydride is the dominant or only phase. This is further illustrated by the observation that of five specimens tested with $x = 1.5$, three failed prior to reaching the plastic stage and all of the tests had small load drops in the elastic stage. The deformation curves for the specimens with compositions in the ε phase range are interesting, showing a two-stage plastic deformation stage that was not evident in the corresponding tests carried out under confinement. This is likely because the latter tests were terminated prior to reaching the second work hardening stage.

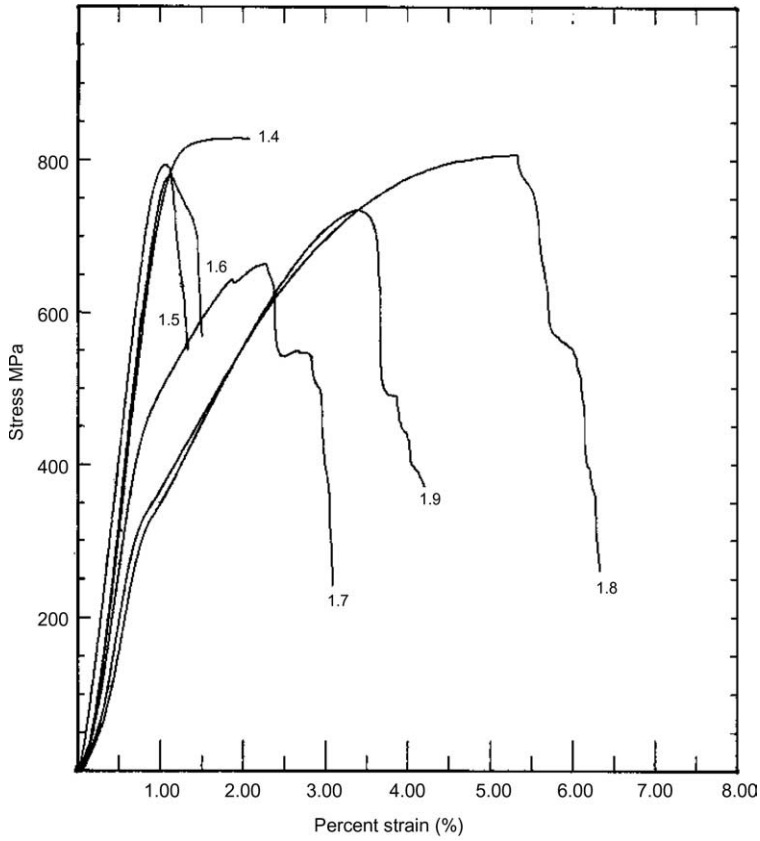

Fig. 9. Examples of stress–strain curves for room temperature, unconfined deformation of solid zirconium hydride. The numbers indicate the stoichiometric composition, $x = H/Zr$, of the hydride.

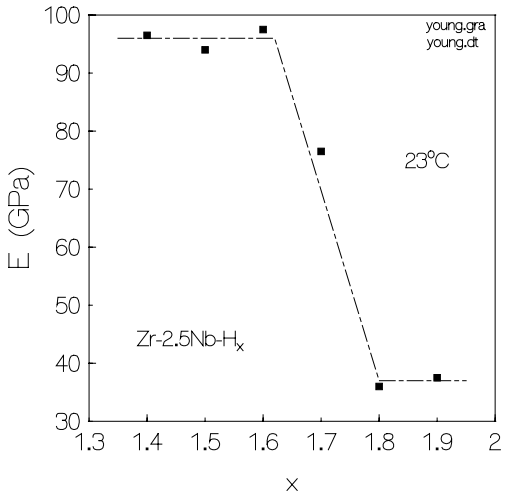

Fig. 10. The Young's modulus, E, of solid hydrides at room temperature from unconfined compression tests. The dashed line has been drawn to indicate the trend.

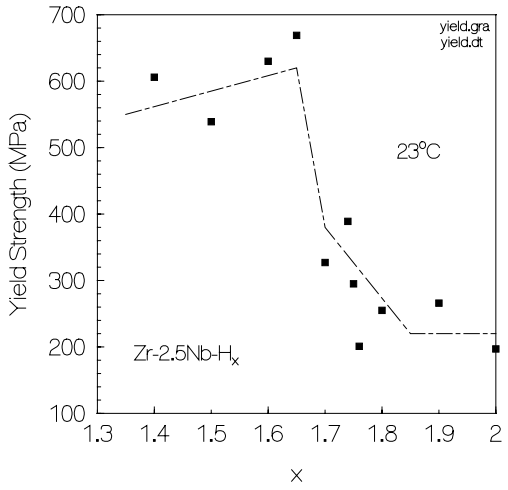

Fig. 11. The yield strength (proportional limit) of solid hydrides at room temperature from unconfined compression tests. The dashed line has been drawn to indicate the trend.

Young's modulus was measured based on the steepest portion of each load–displacement curve and the mean values are plotted in Fig. 10. The overall appearance of the curve of Young's modulus (E) vs. hydrogen compositions is qualitatively consistent with what has been observed in microhardness tests (Fig. 6); there is a significant drop of E in the range from $ZrH_{1.6}$ to $ZrH_{1.8}$, similar also to what was found by Barraclough and Beevers [7] for microhardness. Fig. 11 shows the variation of the yield strengths with x from these specimens. Again, an abrupt drop in the yield strength is observed, starting from when the specimen contains only the δ hydride phase and reaching a minimum level when the specimen contains only the ε hydride phase. It should be noted that the room temperature yield strengths values plotted in Fig. 11 are systematically smaller than the corresponding ones plotted in Fig. 3. This is likely because the latter were tested under confinement.

4. Summary

Young's modulus and yield strength values of solid zirconium hydrides were obtained. These solid hydrides were produced from either a Zr–2.5Nb pressure tube material or from reactor-grade Zr. The mechanical properties of the solid hydride specimens remain almost the same as those of the original pressure tube material for hydrogen compositions up to about $ZrH_{1.6}$. The level of these properties starts to drop when δ hydride becomes the major phase and reaches minimum levels for ε hydrides. Specimens consisting mostly or only of the δ hydride phase have the highest yield strength and lowest ductility. At all compositions, there is a rapid drop in yield strength with temperature from ambient to 150 °C with little further decrease beyond that up to the highest temperature measured of 400 °C.

Acknowledgments

The authors wish to thank A. Stadnyk and B. Ellis, formerly with AECL, Whiteshell Laboratories, for technical assistance in hydrogenating the samples and in carrying out some of the tests, and B.W. Leitch for useful discussions. This work was funded by the CANDU Owners Group (COG) under, successively, WPIR 31-6530 and 31-3108.

References

[1] S.-Q. Shi, M.P. Puls, J. Nucl. Mater. 208 (1994) 232.
[2] S.-Q. Shi, M.P. Puls, in: A.W. Thompson, N.R. Moody (Eds.), Hydrogen Effects in Materials, The Minerals, Metals and Material Society, 1996, p. 611.
[3] K.G. Barraclough, C.J. Beevers, J. Mater. Sci. 4 (1969) 518.
[4] C.J. Beevers, K.G. Barraclough, Mater. Sci. 4 (1969) 802.
[5] P. Veyssière, J. Rabier, M. Jaulin, J.L. Demenet, J. Castaing, Rev. Phys. Appl. 20 (1985) 805.
[6] K.E. Moore, W.A. Young, J. Nucl. Mater. 27 (1968) 316.
[7] K.G. Barraclough, C.J. Beevers, J. Nucl. Mater. 34 (1970) 125.